Journal of ELECTRONIC MATERIALS, Vol. 48, No. 4, 2019
https://doi.org/10.1007/s11664-019-06978-1

Piezoelectric and Dielectric Properties of $((K_{0.475}Na_{0.495}Li_{0.03})NbO_3$-$0.003ZrO_2)$/PVDF Composites

KUN YU,[1,3] SHAN HU,[1,2,4] WENDI YU,[1,5] and JUNQIN TAN[1,6]

1.—Faculty of Materials Science and Chemistry, China University of Geosciences, No. 388. Lumo Road, Hongshan District, Wuhan 430074, Hubei, People's Republic of China. 2.—Engineering Research Center of Nano-Geomaterials of Ministry of Education, China University of Geosciences, Wuhan 430074, People's Republic of China. 3.—e-mail: ujo7400673@163.com. 4.—e-mail: hushan@cug.edu.cn. 5.—e-mail: 771267404@qq.com. 6.—e-mail: 1484646698@qq.com

The $(K_{0.475}Na_{0.495}Li_{0.03})$ NbO_3-$0.003ZrO_2$ (KNNL-Z) ceramic was synthesized by the conventional solid-state reaction and (KNNL-Z)/PVDF composites were fabricated by hot-pressing process using polyvinylidene fluoride (PVDF) and KNNL-Z ceramic. The effects of the ceramic content on the crystalline structures, morphology, densities, dielectric and piezoelectric properties of (KNNL-Z)/PVDF 0–3 composites were systemically studied. The KNNL-Z ceramic possesses a perovskite phase with orthorhombic symmetry and the PVDF polymer mainly possesses α, β and γ phases. Interestingly, the incorporation of the ceramic particles can decrease the crystallite size of the PVDF matrix. In addition, the β phase content increases and the α phase decreases when the ceramic particles are added. When the ceramic content increases from 40 wt.% to 80 wt.%, the relative fraction of β phase increases from 47.7% to 53.8%. Successful incorporation of ZrO_2 into the KNN ceramic has been demonstrated by energy-dispersive x-ray spectroscopy and the most elements are homogeneously distributed in the composites. The dielectric and piezoelectric properties are found to be improved with the increase of KNNL-Z content. When 80 wt.% KNNL-Z is added, the dielectric permittivity reaches the value of 272 (100 Hz) at room temperature and the piezoelectric coefficient is 39 pC/N. After 30 days of aging, it is obvious that all the composites present a good stability of their piezoelectric property.

Key words: KNNL-Z, PVDF, 0–3 composite, piezoelectric properties, dielectric properties

INTRODUCTION

Lead-based piezoelectric ceramics had been widely studied and used in electromechanical transducers, sensors, actuators and other electronic devices.[1–4] However, lead-based materials have been restricted in many areas owing to the toxicity. Nowadays, lead-free piezoelectric ceramics have been widely studied. Among various lead-free piezoelectric ceramic materials, potassium sodium niobate $(K_{(1-x)}Na_xNbO_3)$ has many advantages such as high piezoelectric coefficient, no pollution to the environment and high Curie temperature (T_c > 400°C).[5] Recently, Huan et al. successfully fabricated $(K_{0.52}Na_{0.45}Li_{0.03})$ NbO_3-$0.003SnO_2$-$0.003ZrO_2$ ceramic doped with ZrO_2 and SnO_2 by using the conventional solid-state reaction and obtained remarkably high d_{33} value of about 206 pC/N.[6] This high d_{33} value is due to the substitution of Zr and Sn into the A-sites and B-sites of KNN perovskite, resulting in the formation of defect dipoles and low oxygen vacancy concentration. In addition, ZrO_2 as acceptor doping in KNNL-Z ceramic can increase the creation of complex defects capable of pinning the domain wall motion. Previous studies have also confirmed that the densification is

(Received September 14, 2018; accepted January 17, 2019; published online January 31, 2019)

improved by ZrO_2 doping.[7] At present, many researchers improve the electrical properties of ceramic by doping different elements.[8–10] However, friability is a common problem of ceramic materials and restricts their application. Polymer materials have excellent flexibility, and combining the merits of ceramics and polymers can hold tremendous promise for a wide range of applications, especially for electric device miniaturization and energy storage.[11]

The most commonly used polymer is polyvinylidene fluoride (PVDF), which is a widely available flexible ferroelectric and piezoelectric polymer material with an excellent piezoelectric response.[12,13] PVDF is a semi-crystalline polymer existing in five polymorphic forms, namely α, β, γ, δ, and ε.[14–16] Among these, the α phase is not polar (TGTG' dihedral conformation) and the melting process directly results in this phase. The β, γ and δ are all polar phases. The β phase (TTTT conformation) in particular is mostly responsible for the piezoelectric properties of PVDF and has been studied extensively by researchers.

The 0–3 connectivity possesses a good dispersion of filler in the matrix.[17] And the flexibility of the 0–3 composite is higher than that of pure ceramic. In addition, it is well known that the methods of preparation of composites, such as hot-pressing, cold-pressing, compression molding, solvent casting and electrospinning, have a strong influence on their physical properties.[18–21] The hot-pressing method is widely used because of its convenient and efficient operation.

At present, most lead-free piezoelectric composites (KNN ceramic series) are an un-doped KNN ceramic and PVDF. In this study, the KNN ceramic doped with ZrO_2 was prepared by the conventional solid-state reaction, and then the (KNNL-Z)/PVDF composites were fabricated via hot-pressing. Subsequently, a variety of properties and microstructures were systemically investigated.

EXPERIMENTAL

Preparation of KNNL-Z Ceramic Powder

The $0.997(K_{0.475}Na_{0.495}Li_{0.03})$ NbO_3-$0.003ZrO_2$ ceramic powder was prepared by using the conventional solid-state reaction. High-purity oxide and carbonate starting materials, K_2CO_3 (99%), Na_2CO_3 (99.8%), Nb_2O_5 (99.9%), Li_2CO_3 (99%) and ZrO_2 (99%), were dried at 60°C for 24 h and weighed in stoichiometric amounts. The starting materials were mixed in deionized water, then the mixture was continuously stirred using a magnetic stirrer at 100°C. After the water was completely evaporated, the mixture was ball-milled with ethanol and ZrO_2 balls for 8 h in a nylon jar and subsequently calcined at 850°C for 5 h in air atmosphere. The calcined powder was mixed with 5 wt.% polyvinyl alcohol (PVA) as binder, then pressed into disks of 14 mm in diameter and about 1 mm in thickness at 10 MPa. The disks were buried in alumina powder and the PVA was burned off at 650°C for 5 h then sintered at 1080–1120°C for 3 h in ambient atmosphere. The disks were pounded in an agate mortar until they turned into powder.

Preparation of (KNNL-Z)/PVDF Composites

PVDF polymer was purchased from 3F, China. KNNL-Z powder and PVDF were well mixed with different stoichiometric ratios and subsequently dissolved in ethanol to form a mixture which was continuously stirred by using a magnetic stirrer at 500 rpm, and then intensively mixed by ultrasound. After the volatilization of the solvent, the mixture was pounded in an agate mortar until it became a powder which was pressed into disks of 14 mm in diameter and about 1 mm in thickness at 10 MPa. The disks were hot-pressed at 180°C for 10 min. The surfaces of the composites were wiped to remove impurities after cooling to room temperature.

Characterization

The crystal phases were analyzed by x-ray diffraction (XRD) (XRD diffractometer Bruker AXS D8-Focus; Bruker, Germany) with Cu Kα radiation. The fractured surface microstructures were observed by a scanning electron microscope (SEM) (SU-8010; Hitachi, Japan). The FT-IR spectra of the samples were performed by a Fourier infrared spectrometer (NEXUS 670; Thermo Nicolet, USA). The bulk density was measured by a high-precision electronic gravity meter (DE-200 M; DahoMeter, China) using the Archimedes principle. In order to measure the electrical properties, silver paste was coated on both sides of the samples which were kept inside an oven at 80°C for 2 h to form electrodes. The samples were poled in silicon oil bath at 100°C and applied by a DC field of 4–6 kV/mm for 30 min. After aging all the samples for 24 h, the conductivity and dielectric properties were determined using an LCR meter (E4990A; Keysight Technologies, USA). The piezoelectric coefficient was measured by using a quasi-static d_{33}-meter (PM-200; Piezotest, UK) after aging the samples for 1, 5, 10, 15 , 20, 25 and 30 days.

RESULTS AND DISCUSSION

X-ray Structural Studies

Figure 1 represents the XRD patterns of pure PVDF, KNNL-Z powder and the (KNNL-Z)/PVDF composites. The XRD pattern of the pure PVDF reveals a typical semicrystalline structure composed of the α phase [the peaks at 2θ corresponding to 17.4°(100) and 18.5° (020)], the β phase [the peak at 2θ corresponding to 20.1° (110)] and the γ phase [the peaks at 2θ corresponding to 26.5° (022) and 38.6° (211)].[22,23] The pure KNNL-Z specimen shows sharp peaks at 2θ = 22.6°, 31.9°, 45.4°, 46.1°, 51.7° and 56.9° due to the characteristic planes of (100), (110),

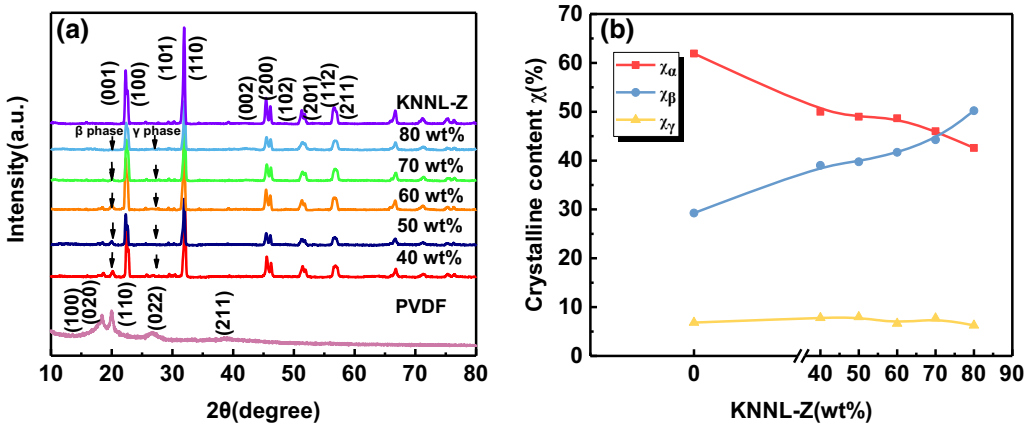

Fig. 1. (a) XRD patterns of pure PVDF, KNNL-Z powder and (KNNL-Z)/PVDF composites. (b) Variation of $\chi_{\alpha,\beta,\gamma}$ with KNNL-Z ceramic content in the composites.

(002), (200), (201) and (211), respectively. This indicates that the KNNL-Z ceramic possesses a pure perovskite phase with orthorhombic symmetry.[24,25] The orthorhombic phase is characterized by the peak at 45.2°(002) which presents a higher intensity compared with the peak at 46.1°(200).[26] The PVDF polymer mainly possesses α, β and γ phases. The β phase is thought to enhance the piezoelectric and ferroelectric properties of the composite.[27,28]

The average crystallite size can be calculated by Scherrer's formula:

$$\text{Crystallite size} = \frac{k\lambda}{\beta_{\text{FWM}}\cos\theta} \tag{1}$$

where k is a shape factor, taken to be 0.89, λ is 0.1542 nm which is the wavelength of the Cu Kα source, θ is the peak position, and β_{FWM} is the full width at half maximum diffraction peak. The crystallite size of the composites is about 16–22 nm. According to Eq. 1, the average crystallite size of the β phase in composites is 17.5, 16.4, 15.6, 15.2 and 14.6, respectively, when their KNNL-Z content are 40–80 wt.%. These results demonstrate that the incorporation of KNNL-Z ceramic particles can decrease the crystallite size of the polymer matrix which contributes to decreasing the energy loss caused by the reversal of the TTTT polymer chains.[29] In order to quantify the crystalline phases of the α, β and γ phases in these composites, the following equation is used:

$$\chi_{\alpha,\beta,\gamma} = \frac{A(\alpha,\beta,\gamma)}{A(\alpha+\beta+\gamma)} \tag{2}$$

where $A(\alpha,\beta,\gamma)$ is the area of characteristic peaks of the α, β or γ phases, and $A(\alpha+\beta+\gamma)$ is the sum of areas of these phases. The variation in the amount of these phases in the PVDF and composites is shown in Fig. 1b from which it can be seen that, when the ceramic content increases, the crystalline content of the β phase improves, but the content of the α phase is restrained. However, the content of the γ phase does not change appreciably. Therefore, the result can be explained by the transformation from the α phase to the β phase. The piezoelectric characteristics of the PVDF polymer are due to the existence of dipoles formed by the carbon bond and fluorine in the structure. When the α phase transforms to the β phase, the strength of the resultant dipole increases so that the piezoelectric response of the PVDF polymer also increases.[30] This transformation makes the composite easier to polarize and to reach higher piezoelectric and dielectric properties.

Micro-structural Characterization

The SEM images of the (KNNL-Z)/PVDF composites are shown in Fig. 2. The particle size of the KNNL-Z ceramic estimated from Fig. 2a–e is approximately 0.5–1.5 μm. The KNNL-Z ceramic can be well dispersed in the three-dimensional interconnected PVDF matrix but the formation of small aggregates at high ceramic content is observed. The (KNNL-Z)/PVDF composites show a typical '0–3' connectivity with a few pores in the fractured surface due to hot-pressing. Successful incorporation of ZrO_2 into the KNN ceramic is demonstrated by EDX. However, the Li element cannot be detected by using the EDX technique due to its light weight. On the whole, it can be seen that most elements are homogeneously distributed in the composites.

EDX mapping results of all the samples, (a1)–(a6), (b1)–(b6), (c1)–(c6), (d1)–(d6) and (e1)–(e6), correspond to the samples in Fig. 2a–e, respectively.

Fourier-Transform Infrared (FTIR) Analysis

Figure 3a shows the FTIR spectra of the pure PVDF and (KNNL-Z)/PVDF composites in the wave number range of 600–1500 cm^{-1}. It can be seen that the characteristic absorption peaks of the α, β and γ phases appear in all the samples. The bands

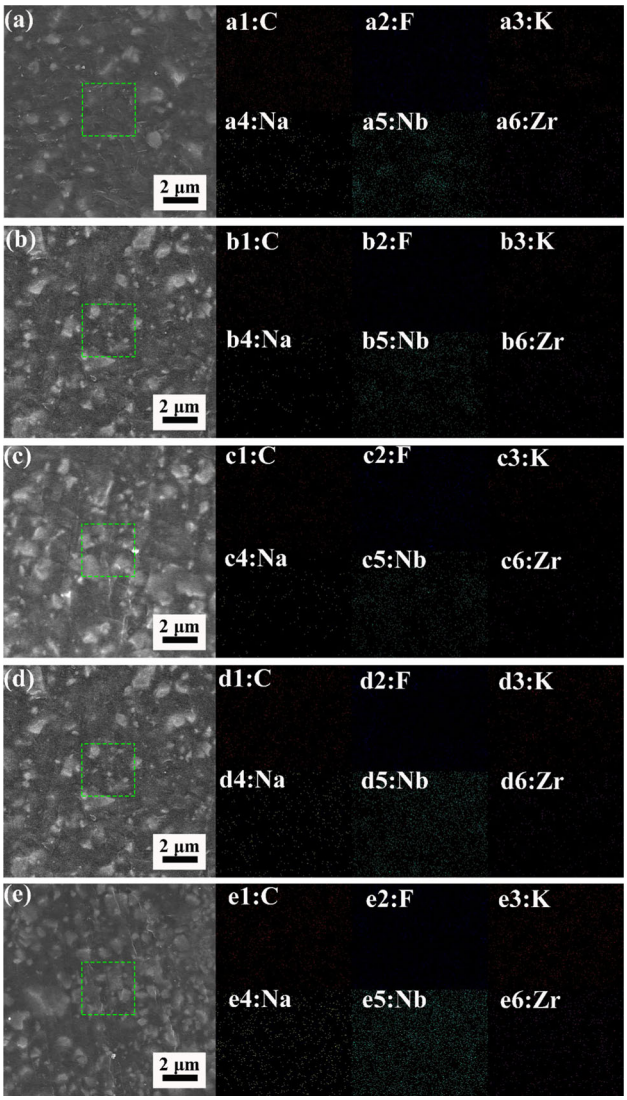

Fig. 2. SEM micrographs of the fractured surfaces of (KNNL-Z)/PVDF composites with KNNL-Z content of (a) 40 wt.%, (b) 50 wt.%, (c) 60 wt.%, (d) 70 wt.%, and (e) 80 wt.%.

identified in the α phase are 614 [CF_2 bending and skeletal bending of C(F)-C(H)-C(F)], 764 [CF_2 bending and skeletal bending of C(F)-C(H)-C(F)], 796 (CH_2 rocking) and 976 cm^{-1} (CH_2 bending mode), which correspond to the TGTG' conformers.[31,32] The bands at 840 (CH_2, CF_2 rocking and asymmetric stretching), 875 (CC skeletal), 1070 (CC skeletal), 1276 (CF_2 skeletal) and 1401 cm^{-1} (CF_2 wagging) are considered to be characteristics of the β phase, which correspond to TTTT chains.[30–33] The band at 834 cm^{-1} is considered to be a signature of the γ phase (C–C stretching), which corresponds to TTTGTTG'.[34,35] All the samples have peaks in essentially the same position, whereas the peaks have different intensities. The FTIR spectra of the composites show that the intensities of most peaks corresponding to the α, β and γ phases decrease compared with that of pure PVDF. Especially, the intensities of the peaks at 614 cm^{-1}, 764 cm^{-1} and 796 cm^{-1} corresponding to the α phase decrease dramatically. The addition of KNNL-Z ceramic particles can influence the relative fraction of the α, β and γ phases in PVDF. In order to evaluate the relative fraction of the β phase in each sample, the following equation is used[36]:

$$F(\beta) = \frac{A_\beta}{1.26A_\alpha + A_\beta} \tag{3}$$

where A_α and A_β are the absorbencies in FTIR spectra corresponding to the 764 cm^{-1} and 840 cm^{-1} bands, respectively. Figure 3b shows the relative fraction of the β phase in the pure PVDF and (KNNL-Z)/PVDF composites. The relative fraction of the β phase is found to be enhanced with the increase of KNNL-Z content, which can be explained by the transformation from the α phase to the β phase. The $F(\beta)$ value of the composite reaches 54% when the KNNL-Z content is 80%. The results arein close agreement with the XRD data (Fig. 1b). Hence, the ceramic particles can increase

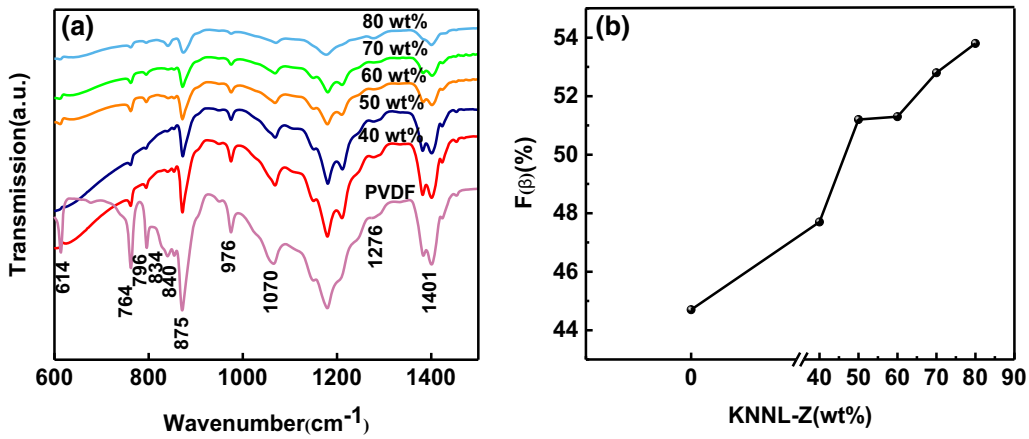

Fig. 3. (a) FTIR spectra of pure PVDF and (KNNL-Z)/PVDF composites. (b) The relative fraction of the β phase in the pure PVDF and (KNNL-Z)/PVDF composites.

the relative fraction of the β phase and enhance the piezoelectric property.

Density

Density is an important physical property of 0–3 composite material. The density of composite material is related to the volume fraction and the density of each component. The volume fraction of KNNL-Z ceramic powder is calculated by Eq. 4:

$$f = \frac{w_c}{w_c + w_p(p_c + p_p)} \quad (4)$$

where f is the volume fraction of the KNNL-Z powder, w_c and p_c are the weight fraction and the experimental density of KNNL-Z ceramic particles, respectively, while w_p and p_p are the weight fraction and the experimental density of PVDF polymer, respectively. The volume fractions of KNNL-Z ceramic powder in the composites are presented in Table I. According to the mixture rule, the theoretical density of this system can be calculated by Eq. 5:

$$\rho_r = \rho_c \times f + \rho_p \times (1 - f) \quad (5)$$

where ρ_r is the theoretical density of the composite, ρ_c and ρ_p are the experimental densities of KNNL-Z and PVDF, respectively. The results are presented in Table I and Fig. 4.

The densities and tightness of the composites are shown in Fig. 4. With the increase of ceramic content, both the experimental density and the theoretical density gradually increase. In addition, the experimental value is always lower than the theoretical value. This phenomenon can be attributed to the existence of some gaps and pores between the ceramic particles and the polymer. Meanwhile, the tightness decreases with the increase of KNNL-Z content, namely, the porosity goes up when the KNNL-Z content increases. However, both the experimental density and the theoretical density increase with decreasing tightness. This can be explained by the fact that the effect of ceramic content on the density is stronger than the porosity on the density.[37] Interestingly, the experimental density can reach approximately 92% or even 97% of the theoretical density at the same ceramic content. Therefore, the experimental density can be predicted accurately by the mixing rule.

Dielectric and Piezoelectric Properties

Figure 5a shows the dielectric permittivity (ε_r) of (KNNL-Z)/PVDF composites as a function of the frequency range from 10^2 Hz to 10^6 Hz at room temperature.

Some studies[12,38] report that the dielectric permittivity decreases with increments of frequency, as in Fig. 5a. This strong frequency dispersion of the dielectric response is the principal characteristic of relaxor ferroelectrics.[39,40] The dielectric permittivity usually keeps a high value at lower frequencies due to electron and ionic displacement polarization, relaxation polarization, dipolar polarization and space charge polarization.[41,42] Among these polarizations, the space charge polarization is the primary reason.[43] As the frequency increases, the relaxation polarization cannot respond to the applied electric field fast enough, which leads to the decrease of dielectric permittivity. And moreover, space charge carriers which play a major role in the space charge polarization require a finite time to align with the direction of an externally applied electric field, and therefore the space charge polarization also decreases with increasing frequency.[44] At higher frequencies, the dipolar polarization and electron displacement polarization can exist while the ionic displacement polarization cannot be maintained because it needs too much time to respond to the applied electric field, and the dipoles play an

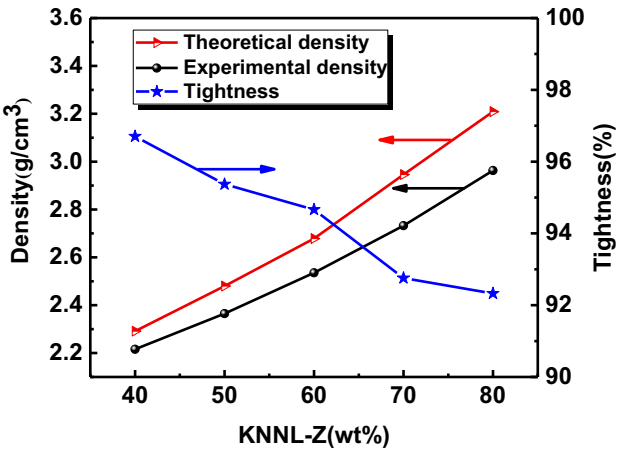

Fig. 4. Variation of the densities and tightness with KNNL-Z ceramic content in the composites.

Table I. Different representation of ceramic contents and densities

Ceramic content (wt.%)	Ceramic content (vol.%)	Experimental density (g/cm^3)	Theoretical density (g/cm^3)
40	24	2.2161	2.2916
50	33	2.3651	2.4799
60	42	2.5356	2.6785
70	53	2.7325	2.9459
80	66	2.9627	3.2089

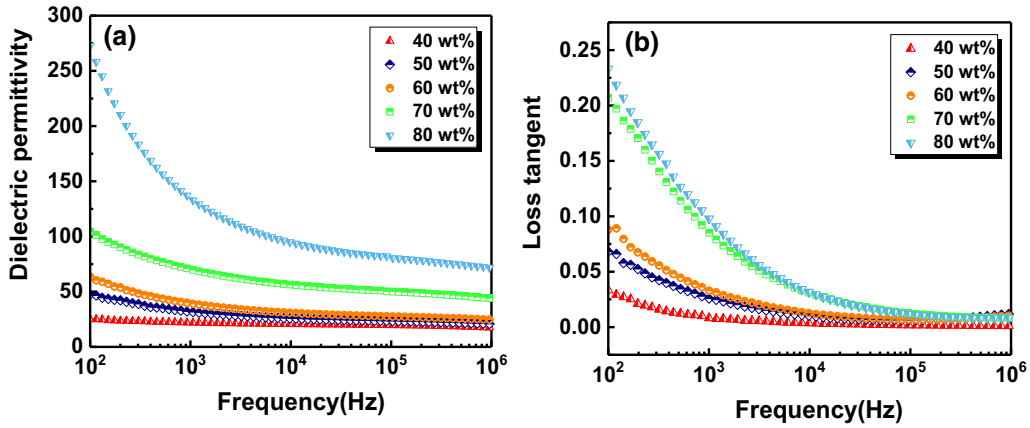

Fig. 5. Frequency dependence of (a) dielectric permittivity and (b) loss tangent of the composites with different weight fractions.

important role in the polarization at higher frequencies.[45] However, because the electron displacement polarization and dipolar polarization begin to lag behind the field, the dielectric permittivity presents a low value at higher frequencies.[46] In addition, since the dielectric permittivity of the KNNL-Z ceramic is much higher than that of the PVDF polymer, it is easy to understand that the dielectric permittivity increases with the increase of ceramic content in the composite at the same frequency.

Figure 5b shows the loss tangent ($\tan\delta$) of (KNNL-Z)/PVDF composites as a function of the frequency range from 10^2 Hz to 10^6 Hz at room temperature. It is observed that the loss tangent keeps a high value in the lower frequencies and has a general trend of decreasing with increments of frequency, indicating the relaxation process.[47] This is due to an accumulation of free charges at lower frequencies and the attenuation of various polarizations at higher frequencies. General speaking, the loss tangent includes two kinds of losses, polarization loss and leakage loss. Therefore, the loss tangent can be expressed as the sum of the two losses. The polarization loss is mainly due to the above polarizations, while the leakage loss is due to leakage current. According to the Kramers–Krönig equation, the loss tangent can be expressed as Eq. 6:

$$\tan\delta = \frac{(\varepsilon_s - \varepsilon_\infty)w\tau}{\varepsilon_s + \varepsilon_\infty w^2\tau^2} + \frac{\gamma}{w\varepsilon_0\varepsilon_r'} \qquad (6)$$

where ε_s is the static dielectric permittivity and ε_∞ is the dielectric permittivity at optical frequencies. w is the angular frequency, τ is the relaxation time, γ is the conductivity of the medium, ε_r' is the real part of the dielectric permittivity, and ε_0 is the permittivity of a vacuum. When the angular frequency w of the electric field is close to 0 or $w\tau \le 1$ at lower frequencies, the polarization loss is close to 0 and only the leakage loss can exist, while the loss tangent tends to infinity. When $w\tau \ge 1$ at higher frequencies, the polarization loss becomes the main

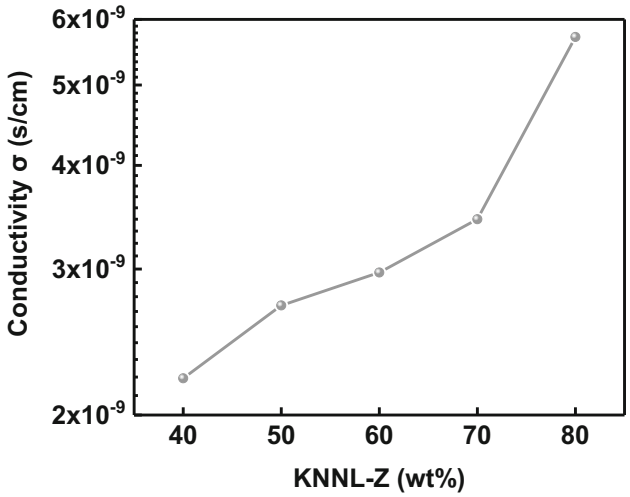

Fig. 6. Variation of the conductivity σ with KNNL-Z content in the composites.

factor causing the loss tangent, which is inversely proportional to the angular frequency. Therefore, the loss tangent decreases with increments of frequency. This strong dispersion in the loss tangent indicates the influence of space charge polarization effects.[48] In addition, the loss tangent increases with the increase of ceramic content in the composite at the same frequency, which may be due to the formation of more micropores at higher content.[49] This inference is also consistent with the phenomenon in which the SEM images are observed (Fig. 2).

When the frequency is 100 Hz, the KNNL-Z ceramic contents are between 40% and 70%, and the dielectric permittivity of the composites does not show a significant change as the ceramic content increases. However, the loss tangent is 0.233 when the KNNL-Z ceramic content is 80%. At this ceramic content, the dielectric permittivity increases significantly and reaches a high value of 272, which is about 29 times higher than that of pure PVDF. Furthermore, the conductivity σ of all the samples is

shown in Fig. 6 and increases with the ceramic content in the composites. It can be clearly seen that, when the weight fraction of the ceramic increases from 70% to 80% (the corresponding volume fractions are given in Table I), the conductivity increases dramatically. This phenomenon of the sharp increases of the dielectric permittivity and the conductivity can be explained by the percolation theory,[50,51] according to which, especially in inorganic–organic composites, the dielectric permittivity of percolative composites follows the formula 7:

$$\varepsilon_r = \varepsilon_m \left| \frac{f_c - f}{f_c} \right|^{-s} \tag{7}$$

where ε_m is the dielectric permittivity of the PVDF matrix, f is the volume fraction of the ceramic, f_c is the percolation threshold, and s is a critical exponent (about 1). Obviously, as f approaches f_c, the dielectric permittivity and the conductivity increase dramatically.

In order to estimate the frequency stability in each sample, the following formula has been used to calculate it[38]:

$$S = \frac{\varepsilon_r(f = 100\ \text{Hz}) - \varepsilon_r(f = 1\ \text{MHz})}{\varepsilon_r(f = 100\ \text{Hz})} \times 100\% \tag{8}$$

The result shows that, when the KNNL-Z content is 40%, 50%, 60%, 70% and 80%, the S is 32%, 57%, 59%, 61% and 64%, respectively, which indicates that the frequency stability of the composite decreases with the increase of KNNL-Z content.

Figure 7 shows the piezoelectric coefficient d_{33}, piezoelectric voltage coefficient g_{33} and the figure-of-merit (FOM) as a function of the weight fraction of the KNNL-Z particles. The value of d_{33} increases with the content of the KNNL-Z ceramic and also corresponds to the analysis of the XRD data and FTIR spectra. It is clearly seen that the composite exhibits a relatively high piezoelectric coefficient, as high as 39 when 80 wt.% ceramic powder was added to the composite. In addition, although d_{33} and g_{33} have different physical meanings, d_{33} and g_{33} are related to each other. The relationship between d_{33} and g_{33} can be described in Eq. 9:

$$g_{33} = \frac{d_{33}}{\varepsilon_{33}^T} \tag{9}$$

where ε_{33}^T is the dielectric permittivity measured at a constant stress, called the 'free' dielectric permittivity. It can be calculated by Eq. 10:

$$\varepsilon_{33}^T = \frac{C^T \times L}{A} \tag{10}$$

where C^T is the capacitance at 1 kHz, A is the electrode area of a sample, and L is the thickness of the specimen. In some ways, $d_{33} \times g_{33}$ can represent a performance of a piezoelectric material for energy harvesting; thus, $d_{33} \times g_{33}$ has been used as a FOM:

$$\text{FOM} = d_{33} \times g_{33} = \frac{d_{33}^2}{\varepsilon_{33}^T} = \frac{d_{33}^2 \times A}{C^T \times L} \tag{11}$$

The FOM reaches the value of 180 when the weight fraction of KNNL-Z is 80%, which is probably due to the better dispersion or smaller trapping of air during blending.

Figure 8 shows the aging characteristic of the d_{33} for all samples from which it can be seen that the d_{33} of all the samples is not changed significantly in 30 days, showing that all the samples have good piezoelectric stability.

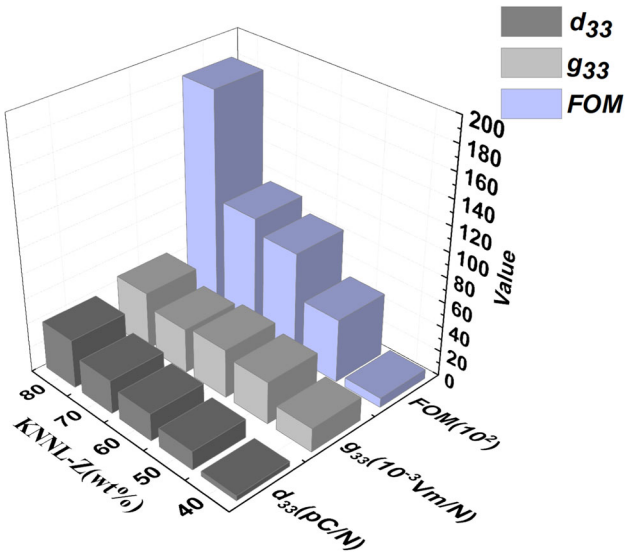

Fig. 7. The d_{33}, g_{33} and FOM of the composites as a function of the weight fraction of KNNL-Z particles.

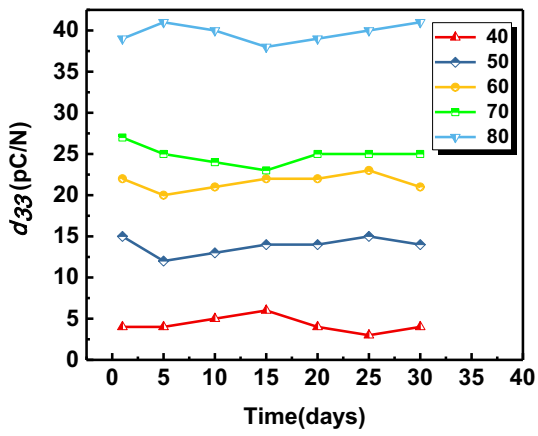

Fig. 8. Dependence of d_{33} of all the samples on time.

CONCLUSION

The $0.997(K_{0.475}Na_{0.495}Li_{0.03})$ NbO_3-$0.003ZrO_2$ ceramic was prepared by the conventional solid-state reaction. Subsequently, the composites were fabricated by the hot-pressing process using KNNL-Z ceramic powder and PVDF polymer. X-ray study confirmed that the XRD pattern of the ceramic is a perovskite phase with orthorhombic symmetry and the PVDF mainly possesses α, β and γ phases. The KNNL-Z ceramic particles can decrease the crystallite size of the PVDF and promote the transformation process of the α phase to the β phase. In addition, ceramic particles can increase the relative fraction of the β phase of the PVDF matrix. When the KNNL-Z ceramic content is 80%, the piezoelectric coefficient can reach 39 pC/N and the composites have good piezoelectric stability. At the same ceramic content, the composite exhibits a dielectric permittivity as high as 272, which is 29 times higher than pure PVDF with a loss tangent as low as 0.233 at 100 Hz. The dielectric properties were well explained in terms of an interfacial percolation model.

ACKNOWLEDGMENT

This work was supported by Science and Technology development Fund of China University of Geosciences (Grant No. 110-KH14J130).

CONFLICT OF INTEREST

The authors declare that there is no conflict of interests regarding the publication of this article.

REFERENCES

1. K. Singh, V. Lingwal, S.C. Bhatt, N.S. Panwar, and B.S. Semwal, *Mater. Res. Bull.* 36, 2365 (2001).
2. H.H. Su, C.S. Hong, C.C. Tsai, S.Y. Chu, and C.S. Lin, *Ceram. Int.* 42, 17558 (2016).
3. J.G. Hao, Z.J. Xu, R.Q. Chu, W. Li, G.R. Li, and Q.R. Yin, *J. Alloy. Compd.* 484, 233 (2009).
4. M. Arbatti, X.B. Shan, and Z.Y. Cheng, *Adv. Mater.* 19, 1369 (2007).
5. L. Wu, J.L. Zhang, C.L. Wang, and J.C. Li, *J. Appl. Phys.* 103, 45 (2008).
6. Y. Huan, X.H. Wang, T. Wei, P.Y. Zhao, J. Xie, Z.F. Ye, and L.T. Li, *J. Eur. Ceram. Soc.* 37, 2057 (2017).
7. G. Leveque, P. Marchet, F. Levassort, L.P. Tran-Huu-Hue, and J.R. Duclere, *J. Eur. Ceram. Soc.* 31, 577 (2011).
8. X. Vendrell, J.E. Garcia, X. Bril, D.A. Ochoa, L. Mestres, and G. Dezanneau, *J. Eur. Ceram. Soc.* 35, 125 (2015).
9. L.Q. Cheng, K. Wang, and J.F. Li, *Mater. Lett.* 138, 128 (2015).
10. L. Ramajo, J. Taub, and M.S. Castro, *J. Mater. Sci. Mater. Electron.* 25, 168 (2014).
11. A. Ameli, M. Nofar, C.B. Park, P. Potschke, and G. Rizvi, *Carbon* 71, 206 (2014).
12. J.Q. Lin, G.R. Chen, W.L. Yang, H. Li, and Q.Q. Lei, *J. Polym. Res.* 23, 143 (2016).
13. R. Senthilkumar, K. Sridevi, J. Venkatesan, V. Annamalai, and M.S. Vijaya, *Ferroelectrics* 325, 121 (2005).
14. Z.L. Cui, N.T. Hassankiadeh, Y.B. Zhuang, E. Drioli, and Y.M. Lee, *Prog. Polym. Sci.* 51, 94 (2015).
15. A. De Neef, C. Samuel, G. Stoclet, M. Rguiti, C. Courtois, P. Dubois, J. Soulestin, and J.M. Raquez, *Soft Matter* 14, 4591 (2018).
16. N. Jahan, F. Mighri, D. Rodrigue, and A. Ajji, *Appl. Clay Sci.* 152, 93 (2018).
17. S.K. Pradhan, A. Kumar, A.N. Sinha, P. Kour, R. Pandey, P. Kumar, and M. Kar, *Ferroelectrics* 516, 18 (2017).
18. B. Ponraj, R. Bhimireddi, and K.B.R. Varma, *J .Adv. Ceram.* 5, 308 (2016).
19. E. Venkatragavaraj, B. Satish, P.R. Vinod, and M.S. Vijaya, *J. Phys. D Appl. Phys.* 34, 487 (2001).
20. D.Q. Zhang, D.W. Wang, J. Yuan, Q.L. Zhao, Z.Y. Wang, and M.S. Cao, *Chin. Phys. Lett.* 25, 4410 (2008).
21. M. Kato and K.I. Kakimoto, *Mater. Lett.* 156, 183 (2015).
22. K. Yu, H. Wang, Y.C. Zhou, Y.Y. Bai, and Y.J. Niu, *J. Appl. Phys.* 113, 321 (2013).
23. A.K. Zak, W.C. Gan, W.H. Abd Majid, M. Darroudi, and T.S. Velayutham, *Ceram. Int.* 37, 1653 (2011).
24. M. Feizpour, H.B. Bafrooei, R. Hayati, and T. Ebadzadeh, *Ceram. Int.* 40, 871 (2014).
25. J. Pavlic, B. Malic, and T. Rojac, *J. Eur. Ceram. Soc.* 34, 285 (2014).
26. T. Lusiola, A. Hussain, M.H. Kim, T. Graule, and F. Clemens, *Actuators* 45, 2344 (2015).
27. P. Kim, S.C. Jones, P.J. Hotchkiss, J.N. Haddock, B. Kippelen, S.R. Marder, and J.W. Perry, *Adv. Mater.* 19, 1001 (2007).
28. S. Chen, K. Yao, F.E.H. Tay, and C.L. Liow, *J. Appl. Phys.* 102, 234 (2007).
29. L.Y. Xie, X.Y. Huang, Y.H. Huang, K. Yang, and P.K. Jiang, *J. Phys. Chem. C* 117, 22525 (2013).
30. I.Y. Abdullah, M. Yahaya, M.H.H. Jumali, and H.M. Shanshool, *Opt. Quantum Electron.* 48, 424 (2016).
31. C.J. Dias and D.K. DasGupta, *IEEE Trans. Dielectr. Electr. Insul.* 3, 706 (1996).
32. T. Greeshma, R. Balaji, and S. Jayakumar, *Ferroelectr. Lett.* 40, 41 (2013).
33. L. Yu and P. Cebe, *Abstr. Pap. Am. Chem. Soc.* 238, 34 (2009).
34. V. Tiwari and G. Srivastava, *Ceram. Int.* 41, 8008 (2015).
35. S. Satapathy, S. Pawar, P.K. Gupta, and K.B.R. Varma, *Bull. Mater. Sci.* 34, 727 (2011).
36. R. Gregorio and N.C.P.D. Nociti, *J. Phys. D Appl. Phys.* 28, 432 (1995).
37. J.H. Seol, J.S. Lee, H.N. Ji, Y.P. Ok, G.P. Kong, K.S. Kim, C.Y. Kim, and W.P. Tai, *Ceram. Int.* 38, 263 (2012).
38. S.T. Wang, J. Sun, L. Tong, Y.M. Guo, H. Wang, and C.C. Wang, *Mater. Lett.* 211, 114 (2018).
39. T. Kar, J. Mal, and R.N.P. Choudhary, *J. Mater. Sci. Lett.* 16, 328 (1997).
40. Z.M. He, J. Ma, R.F. Zhang, and T. Li, *J. Eur. Ceram. Soc.* 23, 1943 (2003).
41. A. Ashok, T. Somaiah, D. Ravinder, C. Venkateshwarlu, C.S. Reddy, K.N. Rao, and M. Prasad, *World J. Condens. Matter Phys.* 2, 257 (2012).
42. E. Atamanik and V. Thangadurai, *J. Phys. Chem. C* 113, 4648 (2009).
43. Y. Chen, S.X. Xie, H.M. Wang, Q. Chen, Q.Y. Wang, J.G. Zhu, and Z.W. Guan, *J. Alloy. Compd.* 696, 746 (2017).
44. N. Marimuthu, R. Parasuraman, M. Rathnakumari, P. Kumar, and R. Upadhyay, *J. Mater. Sci. Mater. Electron.* 29, 1280 (2018).
45. Y. Zhou, J.C. Zhang, L. Li, Y.L. Su, J.R. Cheng, and S.X. Cao, *J. Alloy. Compd.* 484, 535 (2009).
46. K.T. Selvi, K. Alamelumangai, M. Priya, M. Rathnakumari, P.S. Kumar, and S. Sagadevan, *J. Mater. Sci. Mater. Electron.* 27, 6457 (2016).
47. I.S. Elashmawi, E.M. Abdelrazek, H.M. Ragab, and N.A. Hakeem, *Phys. B* 405, 94 (2010).
48. A. Khokhar, P.K. Goyal, O.P. Thakur, and K. Sreenivas, *Ceram. Int.* 41, 4189 (2015).
49. E. Roncari, C. Galassi, F. Craciun, C. Capiani, and A. Piancastelli, *J. Eur. Ceram. Soc.* 21, 409 (2001).

50. Z.M. Dang, L. Wang, Y. Yin, Q. Zhang, and Q.Q. Lei, *Adv. Mater.* 19, 852 (2007).
51. W.H. Yang, S.H. Yu, R. Sun, and R.X. Du, *Acta Mater.* 59, 5593 (2011).